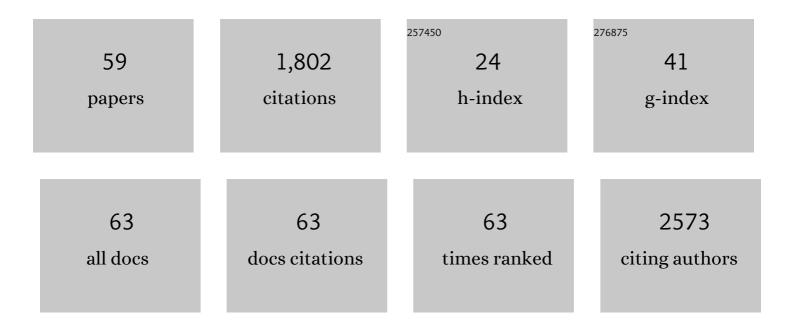
Gerald T Seidler

List of Publications by Year in descending order

Source: https://exaly.com/author-pdf/832087/publications.pdf Version: 2024-02-01



#	Article	IF	CITATIONS
1	Fast and reversible zinc ion intercalation in Al-ion modified hydrated vanadate. Nano Energy, 2020, 70, 104519.	16.0	188
2	Structural engineering of hydrated vanadium oxide cathode by K+ incorporation for high-capacity and long-cycling aqueous zinc ion batteries. Energy Storage Materials, 2020, 29, 9-16.	18.0	139
3	Energy-Degeneracy-Driven Covalency in Actinide Bonding. Journal of the American Chemical Society, 2018, 140, 17977-17984.	13.7	108
4	Enhanced Lithium-Ion Intercalation Properties of V ₂ O ₅ Xerogel Electrodes with Surface Defects. Journal of Physical Chemistry C, 2011, 115, 4959-4965.	3.1	96
5	Probing Surface Defects of InP Quantum Dots Using Phosphorus Kα and Kβ X-ray Emission Spectroscopy. Chemistry of Materials, 2018, 30, 6377-6388.	6.7	70
6	An improved laboratory-based x-ray absorption fine structure and x-ray emission spectrometer for analytical applications in materials chemistry research. Review of Scientific Instruments, 2019, 90, 024106.	1.3	70
7	Interface Engineering V ₂ O ₅ Nanofibers for Highâ€Energy and Durable Supercapacitors. Small, 2019, 15, e1901747.	10.0	66
8	Covalency in Metal–Oxygen Multiple Bonds Evaluated Using Oxygen K-edge Spectroscopy and Electronic Structure Theory. Journal of the American Chemical Society, 2013, 135, 1864-1871.	13.7	57
9	Tailoring Energy and Power Density through Controlling the Concentration of Oxygen Vacancies in V ₂ O ₅ /PEDOT Nanocable-Based Supercapacitors. ACS Applied Materials & Interfaces, 2019, 11, 16647-16655.	8.0	57
10	Aminophosphines as Versatile Precursors for the Synthesis of Metal Phosphide Nanocrystals. Chemistry of Materials, 2018, 30, 5373-5379.	6.7	54
11	V ₂ O ₅ –Conductive polymer nanocables with built-in local electric field derived from interfacial oxygen vacancies for high energy density supercapacitors. Journal of Materials Chemistry A, 2019, 7, 17966-17973.	10.3	53
12	Local Electronic Structure of Dicarba- <i>closo</i> -dodecarboranes C ₂ B ₁₀ H ₁₂ . Journal of the American Chemical Society, 2008, 130, 925-932.	13.7	50
13	Effect of pore morphology on the electrochemical properties of electric double layer carbon cryogel supercapacitors. Journal of Applied Physics, 2008, 104, 014305.	2.5	46
14	New Insights into the Highâ€Performance Black Phosphorus Anode for Lithiumâ€Ion Batteries. Advanced Materials, 2021, 33, e2101259.	21.0	41
15	Competing Effects of Fluorination on the Orientation of Aromatic and Aliphatic Phosphonic Acid Monolayers on Indium Tin Oxide. Journal of Physical Chemistry C, 2013, 117, 15139-15147.	3.1	40
16	A compact dispersive refocusing Rowland circle X-ray emission spectrometer for laboratory, synchrotron, and XFEL applications. Review of Scientific Instruments, 2017, 88, 073904.	1.3	40
17	The coordination chemistry of Cm ^{III} , Am ^{III} , and Ac ^{III} in nitrate solutions: an actinide L ₃ -edge EXAFS study. Chemical Science, 2018, 9, 7078-7090.	7.4	40
18	Experimental and Theoretical Comparison of the O K-Edge Nonresonant Inelastic X-ray Scattering and X-ray Absorption Spectra of NaReO4. Journal of the American Chemical Society, 2010, 132, 13914-13921.	13.7	37

GERALD T SEIDLER

#	Article	IF	CITATIONS
19	X-ray Emission Spectroscopy of Biomimetic Mn Coordination Complexes. Journal of Physical Chemistry Letters, 2017, 8, 2584-2589.	4.6	31
20	Probing Sulfur Chemical and Electronic Structure with Experimental Observation and Quantitative Theoretical Prediction of Kα and Valence-to-Core Kβ X-ray Emission Spectroscopy. Journal of Physical Chemistry A, 2020, 124, 5415-5434.	2.5	30
21	Intermediate-range order in water ices: Nonresonant inelastic x-ray scattering measurements and real-space full multiple scattering calculations. Physical Review B, 2009, 79, .	3.2	26
22	Conjugated Metal–Organic Macrocycles: Synthesis, Characterization, and Electrical Conductivity. Journal of the American Chemical Society, 2022, 144, 4515-4521.	13.7	25
23	<mml:math <br="" xmlns:mml="http://www.w3.org/1998/Math/MathML">display="inline"><mml:mrow><mml:mn>4</mml:mn><mml:mi>f</mml:mi></mml:mrow></mml:math> electron delocalization and volume collapse in praseodymium metal. Physical Review B, 2012, 85, .	3.2	24
24	Kinetic Modeling of the X-ray-Induced Damage to a Metalloprotein. Journal of Physical Chemistry B, 2013, 117, 9161-9169.	2.6	24
25	Benchtop Nonresonant X-ray Emission Spectroscopy: Coming Soon to Laboratories and XAS Beamlines Near You?. Journal of Physics: Conference Series, 2016, 712, 012036.	0.4	24
26	X-ray Emission Spectroscopy of Mn Coordination Complexes Toward Interpreting the Electronic Structure of the Oxygen-Evolving Complex of Photosystem II. Journal of Physical Chemistry C, 2016, 120, 3326-3333.	3.1	24
27	Sulfur Speciation in Biochars by Very High Resolution Benchtop Kα X-ray Emission Spectroscopy. Journal of Physical Chemistry A, 2018, 122, 5153-5161.	2.5	24
28	Rapid Evolution of the Photosystem II Electronic Structure during Water Splitting. Physical Review X, 2018, 8, .	8.9	23
29	Determination of Hexavalent Chromium Fractions in Plastics Using Laboratory-Based, High-Resolution X-ray Emission Spectroscopy. Analytical Chemistry, 2018, 90, 6587-6593.	6.5	23
30	Unsupervised machine learning for unbiased chemical classification in X-ray absorption spectroscopy and X-ray emission spectroscopy. Physical Chemistry Chemical Physics, 2021, 23, 23586-23601.	2.8	23
31	Surface Functionalization of Black Phosphorus with Nitrenes: Identification of P=N Bonds by Using Isotopic Labeling. Angewandte Chemie - International Edition, 2021, 60, 9127-9134.	13.8	21
32	Robust optic alignment in a tilt-free implementation of the Rowland circle spectrometer. Journal of Electron Spectroscopy and Related Phenomena, 2017, 215, 8-15.	1.7	20
33	Laboratory-Based X-ray Absorption Spectroscopy on a Working Pouch Cell Battery at Industrially-Relevant Charging Rates. Journal of the Electrochemical Society, 2019, 166, A2549-A2555.	2.9	20
34	Real-space Green's function calculations of Compton profiles. Physical Review B, 2012, 85, .	3.2	19
35	Reducing radiation damage in macromolecular crystals at synchrotron sources. Acta Crystallographica Section D: Biological Crystallography, 2009, 65, 366-374.	2.5	16
36	A color x-ray camera for 2–6 keV using a mass produced back illuminated complementary metal oxide semiconductor sensor. Review of Scientific Instruments, 2018, 89, 093111	1.3	14

3

GERALD T SEIDLER

#	Article	IF	CITATIONS
37	A mail-in and user facility for X-ray absorption near-edge structure: the CEI-XANES laboratory X-ray spectrometer at the University of Washington. Journal of Synchrotron Radiation, 2019, 26, 2086-2093.	2.4	14
38	Direct Measurement of Acceptor Group Localization on Donor–Acceptor Polymers Using Resonant Auger Spectroscopy. Journal of Physical Chemistry C, 2014, 118, 5570-5578.	3.1	13
39	Vacuum formed temporary spherically and toroidally bent crystal analyzers for x-ray absorption and x-ray emission spectroscopy. Review of Scientific Instruments, 2019, 90, 013106.	1.3	12
40	Theoretical treatments of the bound-free contribution and experimental best practice in X-ray Thomson scattering from warm dense matter. Physics of Plasmas, 2013, 20, .	1.9	10
41	Warm dense crystallography. Physical Review B, 2016, 93, .	3.2	10
42	Double-ionization satellites in the x-ray emission spectrum of Ni metal. Physical Review A, 2017, 96, .	2.5	10
43	Valence-to-core X-ray emission spectroscopy of vanadium oxide and lithiated vanadyl phosphate materials. Journal of Materials Chemistry A, 2020, 8, 16332-16344.	10.3	10
44	4â€1: Invited Paper: Role of Phosphorus Oxidation in Controlling the Luminescent Properties of Indium Phosphide Quantum Dots. Digest of Technical Papers SID International Symposium, 2018, 49, 21-24.	0.3	8
45	X-ray Emission Spectroscopy at X-ray Free Electron Lasers: Limits to Observation of the Classical Spectroscopic Response for Electronic Structure Analysis. Journal of Physical Chemistry Letters, 2019, 10, 441-446.	4.6	8
46	Note: A disposable x-ray camera based on mass produced complementary metal-oxide-semiconductor sensors and single-board computers. Review of Scientific Instruments, 2015, 86, 086107.	1.3	7
47	Informed Chemical Classification of Organophosphorus Compounds via Unsupervised Machine Learning of X-ray Absorption Spectroscopy and X-ray Emission Spectroscopy. Journal of Physical Chemistry A, 2022, 126, 4862-4872.	2.5	7
48	Factors Defining the Intercalation Electrochemistry of CaFe ₂ O ₄ -Type Manganese Oxides. Chemistry of Materials, 2020, 32, 8203-8215.	6.7	6
49	Reactivity of a Chloride Decorated, Mixed Valent Ce ^{III/IV} ₃₈ –Oxo Cluster. Inorganic Chemistry, 2022, 61, 193-205.	4.0	6
50	Resonant inelastic X-ray scattering using a miniature dispersive Rowland refocusing spectrometer. Journal of Synchrotron Radiation, 2020, 27, 446-454.	2.4	5
51	X-ray absorption spectroscopy of trivalent Eu, Gd, Tb, and Dy chlorides and oxychlorides. Journal of Alloys and Compounds, 2022, 897, 162629.	5.5	4
52	Effect of chlorine and chromium on sulfur solubility in Lowâ€activity waste glass. International Journal of Applied Glass Science, 0, , .	2.0	3
53	Nonlocal heat transport and improved target design for x-ray heating studies at x-ray free electron lasers. Physical Review B, 2018, 97, .	3.2	2
54	An exploration of benchtop Xâ€ray emission spectroscopy for precise characterization of the sulfur redox state in cementitious materials. X-Ray Spectrometry, 2022, 51, 151-162.	1.4	2

GERALD T SEIDLER

#	Article	IF	CITATIONS
55	Spherically bent mica analyzers as universal dispersing elements for Xâ€ray spectroscopy. X-Ray Spectrometry, 2020, 49, 493-501.	1.4	1
56	Characterizing Polyoxovanadateâ€Alkoxide Clusters Using Vanadium Kâ€Edge Xâ€Ray Absorption Spectroscopy. Chemistry - A European Journal, 2021, 27, 1592-1597.	3.3	1
57	EFFECT OF PORE MORPHOLOGY ON THE ELECTROCHEMICAL PROPERTIES OF ELECTRIC DOUBLE LAYER CARBON CRYOGEL SUPERCAPACITORS. , 2008, , .		Ο
58	Surface Functionalization of Black Phosphorus with Nitrenes: Identification of P=N Bonds by Using Isotopic Labeling. Angewandte Chemie, 2021, 133, 9209-9216.	2.0	0
59	Iron redox analysis of silicate-based minerals and glasses using synchrotron X-ray absorption and laboratory X-ray emission spectroscopy. Journal of Non-Crystalline Solids, 2022, 577, 121326.	3.1	0